A functional role for the 'fibroblast-like cells' in gastrointestinal smooth muscles

Masaaki Kurahashi, Haifeng Zheng, Laura Dwyer, Sean M. Ward, Sang Don Koh and Kenton M. Sanders

Department of Physiology and Cell Biology, University of Nevada School of Medicine, Reno, NV 89557, USA

Non-technical summary Smooth muscles, as in the gastrointestinal tract, are composed of several types of cells. Gastrointestinal muscles contain smooth muscle cells, enteric neurons, glial cells, immune cells, and various classes of interstitial cells. One type of interstitial cell, referred to as 'fibroblast-like cells' by morphologists, are common, but their function is unknown. These cells are found near the terminals of enteric motor neurons, suggesting they could have a role in generating neural responses that help control gastrointestinal movements. We used a novel mouse with bright green fluorescent protein expressed specifically in the fibroblast-like cells to help us identify these cells in the mixture of cells obtained when whole muscles are dispersed with enzymes. We isolated these cells and found they respond to a major class of inhibitory neurotransmitters – purines. We characterized these responses, and our results provide a new hypothesis about the role of fibroblast-like cells in smooth muscle tissues.

Abstract Morphologists have described 'fibroblast-like cells' (FLCs) in smooth muscles. In the gastrointestinal tract, FLCs are distributed along processes of enteric motor neurons and between the circular and longitudinal muscle layers. They are close to nerve varicosities and make gap junctions with smooth muscle cells. They are labelled with antibodies for platelet derived growth factor receptor α (PDGFRα) and small conductance Ca^{2+}-activated K^+ (SK3) channels. We used transgenic mice with constitutive expression of enhanced green fluorescent protein (eGFP) in PDGFRα^+ cells to isolate and study the function of PDGFRα^+ cells as possible mediators of purinergic neurotransmission. PDGFRα^+ cells expressed purine receptors (P2Y1) and SK3 channels abundantly. Under whole cell voltage clamp some PDGFRα^+ cells generated large amplitude spontaneous transient outward currents that were blocked by apamin (300 nM). Dialysis of cells with Ca^{2+} (500 nM) activated large amplitude K^+ currents that were also blocked by apamin. Application of adenosine triphosphate (ATP), adenine diphosphate (ADP) or β-nicotinamide adenine dinucleotide (β-NAD) (1–1000 μM) activated large amplitude, apamin-sensitive K^+ currents in PDGFRα^+ cells that were blocked by the P2Y1 antagonist MRS2500 (1 μM). Responses to purines were not elicited in smooth muscle cells under equivalent conditions, and only very small outward currents were elicited under optimized conditions (e.g. permeabilized patches and high concentrations of ATP; 1 mM). These data show that PDGFRα^+ cells are a novel class of excitable cells with large current densities attributable to SK channels and the molecular and ionic apparatus to mediate enteric inhibitory responses to purines in GI muscles.

This paper is dedicated to the memory of Professor Mollie Homan (1930–2010). Professor Holman was a pioneer in studies of the autonomic and enteric nervous systems and neural control of visceral smooth muscles. Her recordings were the first records of the postjunctional electrical responses to enteric inhibitory neurotransmission (see reference in this paper), and her work is fundamental to the hypotheses and results of the present study.

DOI: 10.1113/jphysiol.2010.201129

(Received 19 October 2010; accepted after revision 13 December 2010; first published online 20 December 2010)
Corresponding author K. M. Sanders: Department of Physiology and Cell Biology, University of Nevada School of Medicine, Reno, NV 89557, USA. Email: ksanders@medicine.nevada.edu

Abbreviations ChTX, charybdotoxin; CM, circular muscle; FLC, fibroblast-like cell; GI, gastrointestinal; ICC, interstitial cell of Cajal; IJP, inhibitory junction potential; LM, longitudinal muscle; nNOS, neuronal nitric oxide synthase; PDGFRα, platelet derived growth factor receptor α; PGP9.5, protein gene product 9.5; P2Y1, purinergic receptor P2Y1; SMC, smooth muscle cell; vAChT, vesicular acetylcholine transporter.

Introduction

Smooth muscles are complex tissues composed of many cell types, including myocytes, nerve cells and/or processes, glial cells and several types of cells identified as interstitial cells. Some interstitial cells have hematopoietic origins and are likely to be involved in innate immune responses, but other cells, such as interstitial cells of Cajal (ICC), are derived from mesenchymal precursors and provide important regulatory functions (Sanders, 1996). There are also interstitial cells referred to as 'fibroblast-like cells' (FLCs), which are distributed in many smooth muscles, such as the tunica muscularis of gastrointestinal (GI) muscles. In GI muscles FLCs have intriguing anatomical distributions mirroring the distribution of ICC (Komuro *et al.* 1999; Iino *et al.* 2009). Anatomists have speculated about the role of FLCs in smooth muscles, but little is known about the involvements of these cells in physiology or disease because no method has been developed to isolate and study their function.

FLCs have ultrastructural features distinct from ICC. The cytoplasm of FLCs has moderate to high electron density, and well-developed rough endoplasmic reticulum (Horiguchi & Komuro, 2000). FLCs do not display basal lamina or caveolae, but form gap junctions with circular and longitudinal smooth muscle cells (SMCs). The sialomucin cell adhesion protein, CD34, has been used to distinguish FLCs from ICC with fluorescence microscopy; however, labelling does not seem robust (Vanderwinden *et al.* 1999, 2000) and CD34 is expressed by many cells. Recently, robust and specific labelling of FLCs with antibodies for platelet-derived growth factor receptor α (PDGFRα) was demonstrated (Iino *et al.* 2009). Cells with PDGFRα-like immunoreactivity (PDGFRα-LI) were distinct from ICC, as shown by double labelling with c-Kit antibodies.

FLCs also express the small-conductance Ca^{2+}-activated K^+ channel protein (SK3) as shown by immunohistochemistry (Klemm & Lang, 2002; Vanderwinden *et al.* 2002; Fujita *et al.* 2003; Iino & Nojyo, 2009). This is intriguing because at present it is unclear which cells mediate the purineric component of enteric inhibitory control of GI motility. SK3 channels and purinergic inhibitory junction potentials (IJPs) in the GI tract are blocked by apamin (Banks *et al.* 1979; Blatz & Magleby, 1986; Gallego *et al.* 2006; Mutafova-Yambolieva *et al.* 2007). SK channels (mainly SK2; Ro *et al.* 2001) and responses to purine agonists have been reported in SMCs (Vogalis & Goyal, 1997; Koh *et al.* 1997; Bayguinov *et al.* 2000), but responses to ATP are often mixed, and in some cases net inward currents, rather than outward currents, which would be necessary for purinergic responses in whole muscles, are elicited (Lee *et al.* 2005; Monaghan *et al.* 2006). Apamin-sensitive IJPs are preserved, if not enhanced, in muscles of W/W^V mice which have greatly reduced ICC-IM (Burns *et al.* 1996; Sergeant *et al.* 2002). These observations suggest that neither SMCs nor ICC may be the primary site of transduction for purinergic motor neurotransmission.

Here we used a mouse model engineered to express eGFP in cells expressing PDGFRα (Hamilton *et al.* 2003). Cells with eGFP were isolated, tested for expression of P2Y1 receptors and SK3 channels, and studied via patch clamp for responses to purinergic agonists. Robust outward currents were evoked in PDGFRα^+ cells (FLCs), but currents of far less density were evoked in SMCs under the same conditions. Our data suggest that purinergic inhibitory neurotransmission may be transduced by PDGFRα^+ cells in GI muscles. This is the first report of a physiological role for PDGFRα^+ cells in smooth muscles.

Methods

Isolation of PDGFRα^+ cells

Pdgfra$^{tm11(EGFP)Sor}$/J heterozygote mice and wild-type siblings (C57BL/6) were obtained from The Jackson Laboratory (Bar Harbor, ME, USA). Animals (3–6 weeks *post partum*) were anaesthetized by isoflurane (AErrane; Baxter, Deerfield, IL, USA) and killed by cervical dislocation. The abdomens were opened and colons were removed and washed with Krebs–Ringer bicarbonate solution as previously described (Koh *et al.* 1997). Mice were maintained and experiments were performed in accordance with the National Institutes of Health *Guide for the Care and Use of Laboratory Animals* and the Institutional Animal Use and Care Committee at the University of Nevada.

Colonic muscles were equilibrated in Ca^{2+}-free Hanks' solution and cells were dispersed as previously described (Koh *et al.* 1997; Zhu *et al.* 2009). The resulting cell suspension was plated onto murine collagen-coated (2.5 μg ml^{-1}, Falcon/BD) glass coverslips in 35 mm culture dishes. The cells were allowed to settle for 10 min before adding culture medium SMGM (Clonetics Corp., San Diego, CA, USA). The cells were incubated at 37°C in a 95% O_2–5% CO_2 incubator for 1–5 h.

Electrophysiological experiments

Voltage clamp. Cells on coverslips were placed in a 300 μl chamber mounted on an inverted microscope. PDGFRα^+ cells were identified by the fluorescence of eGFP in cell nuclei. Whole-cell (dialysed and perforated patches using amphotericin B) and excised, inside-out patch configurations of the patch-clamp technique were used to record membrane currents under voltage clamp. Pipette tip resistances ranged from 3 to 6 MΩ for whole-cell recordings and 5 to 10 MΩ for single channel recordings. An Axopatch 200B amplifier with a CV-4 headstage (Molecular Devices, Sunnyvale, CA, USA) was used to measure ionic currents and membrane potentials. All data were analysed using clampfit (pCLAMP v. 9.2, Molecular Devices) and Graphpad Prism (v. 3.0,Graphpad Software Inc., San Diego, CA, USA).

Solutions and reagents for patch clamp experiments. External solutions for whole-cell recordings included: (i) Ca^{2+}-containing physiological salt solution (CaPSS) containing (mM): 5 KCl, 135 NaCl, 2 $CaCl_2$, 10 glucose, 1.2 $MgCl_2$, and 10 Hepes adjusted to pH 7.4 with Tris, and (ii) Mn^{2+}-containing physiological salt solution (MnPSS), the same as solution (i) but with Ca^{2+} replaced with equimolar Mn^{2+}. The pipette solutions were (mM), solution 1: 135 KCl, 3 MgATP, 0.1 NaGTP, 2.5 creatine phosphate disodium, 0.1 EGTA, 10 Hepes adjusted to pH 7.2 with Tris; and solution 2, high Ca^{2+} (500 nM) pipette solution: 135 KCl, 7.74 $CaCl_2$, 3 MgATP, 0.1 NaGTP, 2.5 creatine phosphate disodium, 10 EGTA, 10 Hepes adjusted to pH 7.2 with Tris. For perforated whole-cell experiments, the pipette solution was (mM): 140 KCl, 0.1 EGTA, and 5 Hepes adjusted to pH 7.2 with Tris. Amphotericin B (1.5 mg/25 μl, Sigma-Aldrich Corp., St Louis, MO, USA) was dissolved with dimethyl sulfoxide, sonicated and diluted in the pipette solution to give a final concentration of 300 μg ml^{-1}. For single channel recordings, the pipette solution and external solution were (mM): 140 KCl, 10 EGTA, 10 Hepes, adjusted to pH 7.2 with Tris. Free Ca^{2+} concentrations were calculated by Maxchelator software (http://maxchelator.stanford.edu). Adenosine 5′-triphosphate magnesium salt (ATP), adenosine 5′-diphosphate sodium salt (ADP), β-nicotinamide adenine dinucleotide hydrate and charybdotoxin were obtained from Sigma-Aldrich. MRS2500 and apamin were obtained from Tocris Bioscience (Ellisville, MO, USA).

Statistical analyses. Data are expressed as means ± S.E.M. of n cells. All statistical analyses were performed using Graphpad Prism. We used Student's paired or non-paired t test to compare groups of data. In all statistical analyses, $P < 0.05$ was considered statistically significant.

Immunohistochemistry

Whole-mount specimens of mouse tissue. Colonic muscles were fixed in acetone (10 min at 4°C – wild-type mice) or paraformaldehyde (4% w/v in 0.1 M PBS; 10 min at 4°C – transgenic mice to preserve eGFP). Following fixation, preparations were washed in phosphate-buffered saline (PBS; 0.01 M, pH 7.4) and non-specific binding was reduced by incubating tissues with 1% bovine serum albumin (BSA) for 1 h. The tissues were incubated with primary antibody for 48 h at 4°C and with secondary antibodies for 1 h at room temperature. Antibodies and dilutions used are shown in Table 1.

Dispersed cells were fixed in paraformaldehyde (4% w/v in 0.1 M PBS for 10 min at 4°C) and washed in 0.01 M PBS. After pre-incubation with 1% BSA for 1 h, cells were incubated in the primary antibody for 30 min at room temperature. Secondary antibody incubations were performed for 15 min at room temperature.

Specimens and dispersed cells were examined with a confocal microscope (Zeiss LSM510 Meta; Carl Zeiss, Thornwood, NY, USA). Micrographs were constructed using Zeiss LSM 5 Image Examiner software, and are composites of Z-series scans (0.2–0.5 μm optical sections) through a depth of 4–40 μm.

Cell purification, RNA isolation, reverse-transcription PCR and quantitative PCR

Cell purification. PDGFRα^+ cells were purified by fluorescence-activated cell sorting (Becton Dickinson FACSAria using the blue laser (488 nm) and the GFP emission detector; 530/30 nm). Cells were further purified by hand collecting of fluorescent cells to maximize purity for molecular tests.

RNA isolation, reverse-transcription PCR and quantitative PCR. Total RNA was isolated from PDGFRα^+ cells using illustra RNAspin Mini RNA Isolation kit (GE Healthcare, Little Chalfont, UK), and first-strand cDNA was synthesized using SuperScript III (Invitrogen, Carlsbad, CA, USA), according to the manufacturer's instructions. PCR was performed with specific primers (Table 2) using AmpliTaq Gold PCR Master Mix (Applied Biosystems,

Table 1. Antibodies

Primary antibodies	Species	Catalogue no.	Dilution	Source
PDGFr α (for acetone fixtative)	Rat	16–1401	1:500	eBioscience, CA, USA
PDGFr α (for 4% PFA fixtative)	Goat	AF1062	1:200	R & D Systems, MN, USA
c-Kit	Goat	AF1356	1:500	R & D Systems, MN, USA
SK3	Rabbit	APC-025	1:500	Alomone Labs, Israel
PGP 9.5	Rabbit	RA-95101	1:500	UltraClone Ltd, UK
nNOS	Sheep		1:200	Gift from Dr Piers Emson, Mol. Sci. Group, Cambridge, UK
vAChT	Goat	ab34852	1:200	Abcam, MA, USA
Secondary antibodies		**Catalogue no.**	**Dilution**	**Source**
Alexa594 labelled donkey anti-rabbit IgG		A-21207	1:500	Molecular Probes/Invitrogen
Alexa488 labelled donkey anti-rat IgG		A-21208	1:500	Molecular Probes/Invitrogen
Alexa488 labelled donkey anti-goat IgG		A-11055	1:500	Molecular Probes/Invitrogen
Alexa594 labelled donkey anti-goat IgG		A-11058	1:500	Molecular Probes/Invitrogen
Alexa594 labelled donkey anti-sheep IgG		A-11016	1:500	Molecular Probes/Invitrogen

Table 2. Primer sequences used for PCR

Gene name	Primer sequence	Product length (bp)	Accession number
Hprt	F- GACTTGCTCGAGATGTCATGAAGGAGAT R- TGTCCCCCGTTGACTGATCATTACAGTA	198	NM_013556.2
Pdgfra	F- ATGACAGCAGGCAGGGCTTCAACG R- CGGCACAGGTCACCACGATCGTTT	195	NM_011058.2
Kit	F- CGCCTGCCGAAATGTATGACG R- GGTTCTCTGGGTTGGGGTTGC	162	NM_021099.2
P2ry1	F- CGGCATCTCCGTGTACATGTTC R- CCTGTGTGCGCTGATGCAGGT	196	NM_008772.4
Kcnn3	F- CTGCTGGTGTTCAGCATCTCTCTG R- GTCCCCATAGCCAATGGAAAGGAAC	150	NM_080466.1

Foster City, CA, USA). PCR products was analysed on 2% agarose gels and visualized by ethidium bromide. Quantitative PCR (qPCR) was performed with the same primers as PCR using Syber green chemistry on the 7300 Real Time PCR System (Applied Biosystems). Regression analysis of the mean values of eight multiplex qPCRs for the log10 diluted cDNA was used to generate standard curves. Unknown amounts of messenger RNA (mRNA) were plotted relative to the standard curve for each set of primers and graphically plotted using Microsoft Excel. This gave transcriptional quantification of each gene relative to the endogenous hypoxanthine guanine phosphoribosyltransferase (*Hprt*) standard after log transformation of the corresponding raw data.

Results

Branching cells with PDGFRα-like immunoreactivity (PDGFRα-LI) were found in the circular muscle (CM) and longitudinal muscle (LM) layers running parallel with the smooth muscle fibres (Fig. 1*A–C*; Supplemental Fig. 1*A–F*), as previously reported (Iino *et al.* 2009). There was also a network of more extensively branching cells with PDGFRα-LI between the CM and LM in the plane of the myenteric plexus (Supplemental Fig. 1*G–I*). PDGFRα^+ cells occupied the same general anatomical spaces and were distributed in similar density as interstitial cells of Cajal (ICC), but PDGFRα^+ cells were distinct from c-Kit$^+$ ICC, as shown by double labelling (Fig. 1*C*; Supplemental Fig. 1*C*, *F* and *I*). ICC have been widely referred to as intramuscular (ICC-IM) and myenteric (ICC-MY) based on their anatomical locations in the tunica muscularis (Sanders, 1996). We suggest that PDGFRα^+-IM and PDGFRα^+-MY are appropriate terms for this new type of interstitial cell in the gastrointestinal tunica muscularis because their anatomical distributions are analogous to ICC.

PDGFRα^+ cells (which previously were termed more vaguely as 'fibroblast-like cells') have been reported to be

immunoreactive for small conductance, Ca^{2+}-activated K^+ channels (i.e. SK3 (Kcnn3); Klemm & Lang, 2002; Vanderwinden *et al.* 2002; Fujita *et al.* 2003; Iino & Nojyo, 2009), and we tested this in double labelling experiments with anti-SK3 antibody. PDGFRα^+-IM in CM (Supplemental Fig. 2*A–C*) and LM and PDGFRα^+-MY (Fig. 1*D–F*, Supplemental Fig. 2*D–I*) co-labelled with SK3 antibodies.

We hypothesized that PDGFRα^+ cells might be involved in transduction of purinergic enteric inhibitory neurotransmission since these cells are often in close apposition with enteric motor nerve varicosities, coupled by gap junctions to SMCs (Horiguchi & Komuro, 2000), and express SK3 channels. We performed double labelling experiments using a neural marker (PGP9.5) and labels for enteric inhibitory (neuronal nitric oxide synthase (nNOS) antibody; Bredt *et al.* 1990; Ward *et al.* 1992) and excitatory (vesicular acetylcholine transporter (vAChT); Weihe *et al.* 1996) motor neurons to determine the proximity of motor neurons and PDGFRα^+ cells. Since there are no data to suggest that purinergic and nitrergic neurons form distinct classes of enteric inhibitory motor neurons, proximity of PDGFRα^+ cells to neural processes with nNOS suggests these cells are closely associated with nerve terminals that release purine neurotransmitters. The distribution of PDGFRα^+ cells in C57BL/6 wild-type (Fig. 1*G–I*; Supplemental Fig. 3*A–C*) and W/W^V (Kit mutants in which ICC are reduced in the colon; Supplemental Fig. 3*D–F*) was grossly indistinguishable. PDGFRα^+ cells in both mouse models were closely associated with inhibitory (nNOS$^+$) and excitatory (vAChT$^+$) enteric motor neurons (Fig. 1*G–I*).

The robust SK3 immunoreactivity of PDGFRα^+ cells suggests these cells may be capable of generating Ca^{2+}-activated K^+ currents, and activation of this conductance could affect excitability of the smooth muscle syncytium due to gap junctions between these cells and SMCs (Horiguchi & Komuro, 2000). If SK channels in PDGFRα^+ cells are activated by purines, then these cells could have a role in mediating the purinergic component of enteric inhibitory neurotransmission. We used a mouse engineered to express a histone 2B–eGFP fusion protein in cells that express PDGFRα to allow identification of PDGFRα^+ cells in mixed cell dispersions. (Hamilton *et al.* 2003). A network of fluorescent cells was observed in GI muscles of these mice, and co-labelling with PDGFRα antibodies demonstrated one-to-one eGFP$^+$ nuclei in PDGFRα^+ cells (Fig. 2*A–C*).

Enzymatic dispersion of colonic muscles from animals with PDGFRα^+ cells labelled with eGFP produced rounded cells with bright green nuclei. These cells co-labelled with PDGFRα antibodies (Fig. 2*D–F*). Dispersed PDGFRα^+ cells had a morphological appearance similar to dispersed ICC (Zhu *et al.* 2009). Therefore, we performed RT-PCR on purified eGFP$^+$ cells. The eGFP$^+$ cells expressed *pdgfra*, *P2ry1* (P2Y1 receptors) and *Kcnn3* (SK3 channels) but not *Kit* (Fig. 2*I*). Thus, we confirmed that the eGFP$^+$ cells were distinct from ICC.

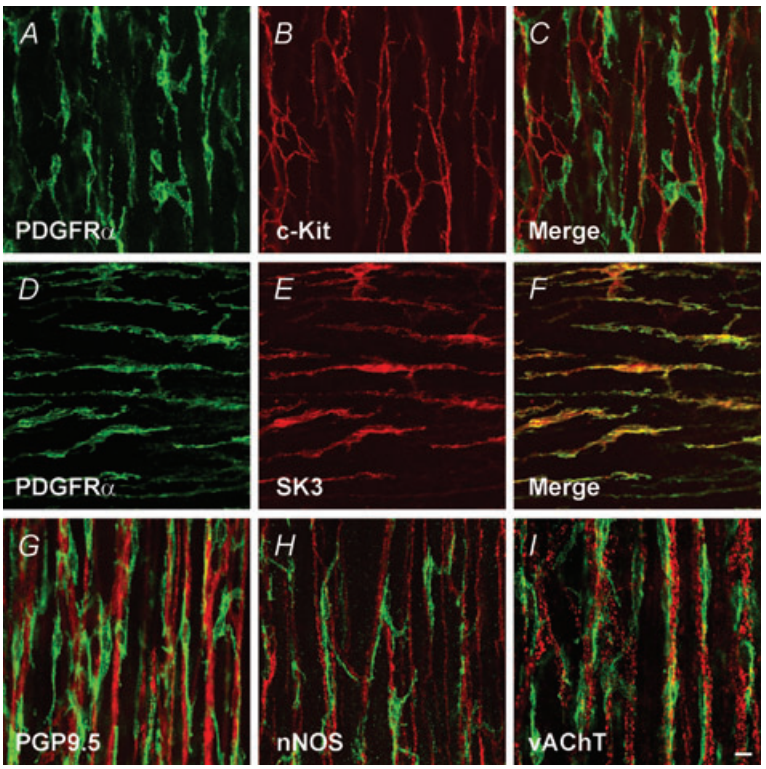

Figure 1. Relation of PDGFRα^+ cells to ICC and enteric neurons
A–C, double immuno-labelling of PDGFRα (green) and c-Kit (red) in circular muscle layer of murine colon. Similar anatomical spaces were occupied by PDGFRα^+ cells and c-Kit$^+$, but no co-labelling of cells was observed demonstrating that these are discrete populations of cells. *D–F*, double immuno-labelling of PDGFRα (green) and SK3 (red) in longitudinal muscle layer of murine colon. PDGFRα^+ cells express small conductance Ca^{2+}-activated K channels (SK3; Iino & Nojyo, 2009). PDGFRα^+ cells in both muscle layers and in the region of the myenteric plexus express SK3. *G–I*, double immuno-labelling of neuronal proteins (red) and PDGFRα (green) in circular muscle layer of murine colon. Red staining in *G*, *H* and *I* shows immunoreactivity for PGP9.5, nNOS and vesicular acetylcholine transporter (vAChT), respectively. PDGFRα^+ cells are closely associated with enteric neurons (PGP9.5) and with specific classes of motor neurons (inhibitory as identified with nNOS antibody and excitatory as identified by vAChT antibody). White bar is 10 μm.

We also performed real time PCR and found that *P2ry1* and *Kcnn3* were strongly expressed by these cells (Fig. 2*J*).

PDGFRα^+ cells were studied with the whole-cell configuration of the patch clamp technique to characterize membrane conductances. Cell membrane capacitance averaged 6.0 ± 0.2 pF ($n = 201$). Dialysis of cells with low Ca^{2+} pipette solution (solution 1) resulted in small amplitude currents in response to step depolarization or ramp protocols from −80 to +80 mV. Step depolarization revealed a small amplitude, time-dependent outward current and a noisy outward current that developed at positive potentials (Fig. 3*A*–*C*). We never observed voltage-dependent inward currents in these cells. The reversal potentials of current responses to ramp potentials averaged -18.1 ± 4.9 mV ($n = 16$ (Fig. 3*D* and *E*), which is positive to the resting membrane potentials of intact colonic muscles (Hwang *et al.* 2009). Dialysis of cells with a solution buffered to contain 500 nM Ca^{2+} (solution 2) resulted in the development of time-independent outward currents averaging 261 ± 135 pA at 0 mV in response to ramp potentials (43.3 ± 22.4 pA pF^{-1}; $n = 6$ cells; Fig. 3*B*–*E*). The reversal potential of these currents shifted toward the equilibrium potential for K^+ ions (−80 mV) and averaged -67.8 ± 3.2 mV), suggesting that elevated internal Ca^{2+} activated a K^+ conductance. The steady-state outward currents that developed in cells dialysed with 500 nM Ca^{2+} were reduced significantly by apamin (300 nM) to 56 ± 34 pA at 0 mV (9 ± 5.6 pA pF^{-1}; $n = 6$; $P < 0.0001$; Fig. 3*D* and *E*). These data suggest that PDGFRα^+ cells express a high density of apamin-sensitive Ca^{2+}-activated K^+ channels, which is consistent with the expression of SK3 channels.

Contribution to the outward current activated by dialysis of cells with 500 nM Ca^{2+} from additional Ca^{2+}-activated K^+ conductances was tested in a further series of experiments. After dialysis of cells and activation

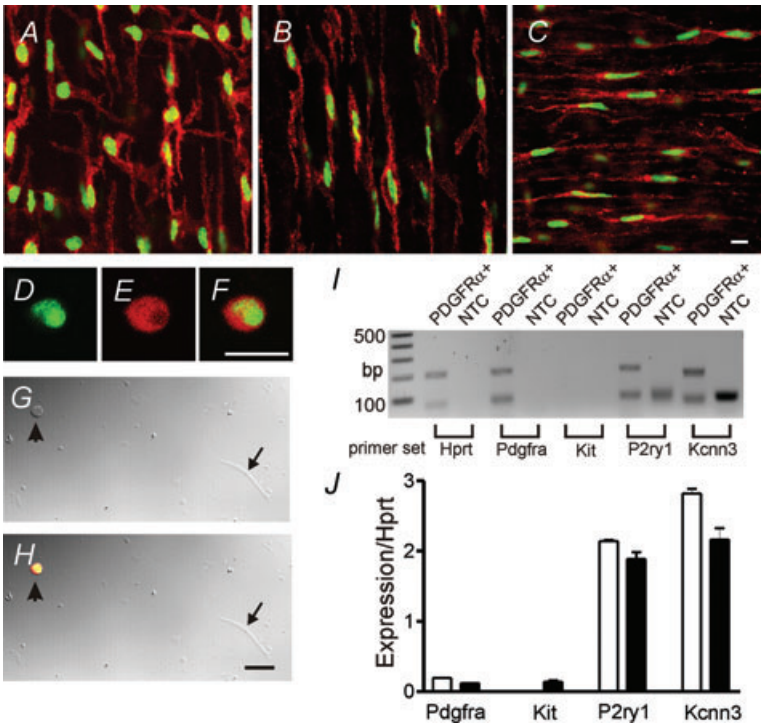

Figure 2. eGFP specifically labels PDGFRα^+ cells
A–*C*, eGFP (green) and PDGFRα-like immunoreactivity (red) co-expressed in PDGFRα^+-MY (*A*), circular muscle PDGFRα^+-IM (*B*) and longitudinal muscle PDGFRα^+-IM (*C*). eGFP is confined to nuclei while PDGFRα is more generally expressed in the plasma membranes. *D*–*F*, eGFP (*D*) and PDGFRα (*E*) are shown in cells dispersed from the colon. Small round nuclei of PDGFRα^+ cells contained eGFP (*F*). *G* and *H*, the same cell is shown with differential interference contrast (DIC) microscopy. PDGFRα^+ cell (arrow head) and a smooth muscle cell (arrow), respectively, were easy to distinguish and smooth muscle cells lacked eGFP expression. White bars and black bar are 10 μm. *I* and *J*, expression of molecular targets for purinergic neurotransmission in sorted PDGFRα^+ cells. Expression analysis was performed by RT-PCR (*I*) and by real-time PCR analysis (*J*) on a highly purified population of PDGFRα^+ cells (see Methods). These cells were not contaminated with Kit-expressing cells (*I*). PDGFRα^+ cells also expressed *P2ry1* (P2Y1 receptors) and *Kcnn3* (SK3 channels). *J* shows relative expression of *Pdgfra*, *Kit*, *P2ry1* and *Kcnn3* as determined by real-time PCR. White bars represent PDGFRα^+ cells and black bars represent whole colon muscle. Note robust expression of *P2ry1* and *Kcnn3* in the PDGFRα^+ cells. *Hprt* is the house-keeping gene, hypoxanthine guanine phosphoribosyl transferase; NTC, non-template control.

of the K^+ conductance noted above, the cells were exposed to charybdotoxin (ChTX; 200 nM), which blocks both large (BK) and intermediate (IK) conductance Ca^{2+}-activated K^+ channels (Ledoux *et al.* 2006). ChTX caused a small, but significant, reduction in outward current at 0 mV from 100 ± 28 pA to 86 ± 23 pA (i.e. 16.6 ± 4.6 pA pF^{-1} to 14.3 ± 3.9 pA pF^{-1} ($P = 0.0488$; $n = 6$; Fig. 3*F* and *G*). Subsequent addition of apamin (300 nM), in the continued presence of ChTX, reduced current to 31 ± 8 pA (5.2 ± 1.3 pA pF^{-1}; $P = 0.0406$; $n = 6$; Fig. 3*F* and *G*).

Some cells held at the approximate physiological resting potential for colonic muscles (−50 mV) displayed large amplitude spontaneous transient outward currents (STOCs) that occurred in clusters (3.2 ± 0.77 per min; 251 ± 83 pA at −50 mV (42 ± 13.8 pA pF^{-1}); $n = 8$ of 418 cells dialysed with solution 1; Fig. 3*H*). STOCs were blocked by apamin (300 nM; Fig. 3*H*). If events of this type occur *in situ*, then STOCs may contribute to resting potentials in intact muscles, and this may explain the depolarization of colonic muscles caused by apamin (Mutafova-Yambolieva *et al.* 2007).

Single channels were characterized in excised patches. Figure 4*A* shows patches stepped from −60 to +20 mV in a symmetrical K^+ gradient (140 mM/140 mM K^+ and 100 nM Ca^{2+}), and current amplitudes (determined from amplitude histograms) are plotted *vs.* potential in Fig. 3*B*. Channels had a unitary conductance of 10 pS, and this is consistent with SK3 channels (Barfod *et al.* 2001). We investigated the Ca^{2+} sensitivity of the channels in excised inside-out (i-o) patches by changing Ca^{2+} at the intracellular surface ($[Ca^{2+}]_i$) from 10^{-8} to 10^{-5} M while ramping potential from −80 to +80 mV (Fig. 4*C*). A plot of normalized current at −60 mV, fitted with a Hill function, is shown in Fig. 4*D*, and the EC_{50} for Ca^{2+}-dependent activation of channels was calculated to be 364 ± 51 nM ($n = 4$), which is consistent with previous reports of the Ca^{2+} sensitivity of SK3 channels (Barfod *et al.* 2001).

Purines (ATP, β-nicotinamide adenine dinucleotide (β-NAD) and ADP) evoked significant outward currents in PDGFRα^+ cells. Figure 5*A* and *C* shows application of ATP (1 mM) and β-NAD (50 μM) during repetitive ramping from −80 to +80 mV under whole-cell recording. In spite of continuous exposure to ATP, current responses reached a maximum averaging 82 ± 27 pA pF^{-1} and then relaxed within 108.1 ± 11.5 s ($\tau_{1/2} = 18.01 \pm 5.12$), suggesting desensitization. Figure 5*B* and *D* shows superimposed current responses to ramps before and at the peak responses. Activation of outward current was concentration dependent (0.1 to 1000 μM; Fig. 6*A* and *B*) and the EC_{50} concentration of ATP was calculated to be 1.96 μM (Fig. 6*B*). The maximum response to ATP was reached at about 10 μM, and responses to lower concentrations of ATP and ADP tended to be STOC-like oscillations in outward current that often exceeded the exposure time to ATP (Fig. 6*A* and *C*). Repetitive exposure to purines resulted in reproducible responses. Figure 6*C* shows alternating application of ATP and ADP (both 10 μM) that activated reproducible current responses. The efficacy of ATP and ADP were similar (Fig. 6*D*).

In colonic muscles purinergic responses are sensitive to apamin and P2Y1 receptor antagonists (Banks *et al.* 1979; Gallego *et al.* 2006; Mutafova-Yambolieva *et al.* 2007). Genes encoding SK3 channels and P2Y1 receptors were expressed in PDGFRα^+ cells (Fig. 2). Therefore, we tested the effects of apamin and MRS2500 on currents elicited in PDGFRα^+ cells by ATP and ADP (both 10 μM, responses to ADP are not illustrated). The purines were administered by rapid infusion repetitively for 20–30 s. At least two control exposures were given to be certain responses were reproducible. Then apamin (300 nM) or MRS2500 (1 μM; P2Y1 antagonist) was administered. Apamin and MRS25000 reduced current amplitudes from 156 ± 35 pA to 47 ± 36 pA (26.0 ± 5.8 pA pF^{-1} to 7.8 ± 6.1 pA pF^{-1}; $n = 6$) and from 225 ± 115 pA to 6 ± 6 pA (37.5 ± 19.2 pA pF^{-1} to 1.0 ± 1.0 pA pF^{-1}; $n = 8$), respectively Fig. 7*A* and *B*).

Responses to purines were Ca^{2+} dependent. After eliciting outward currents with ATP, the extracellular solution was changed to MnPSS, which reduced and blocked responses to ATP (Fig. 8). Purinergic responses recovered after re-addition of CaPSS.

We compared the effects of ATP on smooth muscle cells (SMCs) under the same conditions as tests on PDGFRα^+ cells. In cells dialysed with low Ca^{2+} (solution 1) and at a holding potential of −50 mV, ATP (10 μM–1 mM) had no effect ($n = 19$). To preserve intracellular signalling pathways, we also performed experiments with perforated patch whole cell configuration. ATP (10 μM) had no effect on these cells ($n = 6$); however at 1 mM, ATP either elicited small inward currents ($n = 5$, Fig. 9*A*), outward current ($n = 5$, Fig. 9*B*), or no resolvable response ($n = 14$). In cells with outward current responses, current density at −50 mV and 0 mV was 0.9 ± 0.3 and 2.3 ± 0.4 pA pF^{-1}, respectively.

Discussion

This study shows that PDGFRα^+ cells, referred to for many years as 'fibroblast-like cells' (FLCs), are a novel class of excitable cells in visceral smooth muscles. The arrangement of PDGFRα^+ cells along enteric nerve bundles, close contacts with nerve varicosities (Zhou & Komuro, 1992), and gap junctions with SMCs (Horiguchi & Komuro, 2000) suggest these cells have a role in neurotransmission, because these are essential morphological elements required for PDGFRα^+ cells to transmit neural inputs to the smooth muscle syncytium. We confirmed

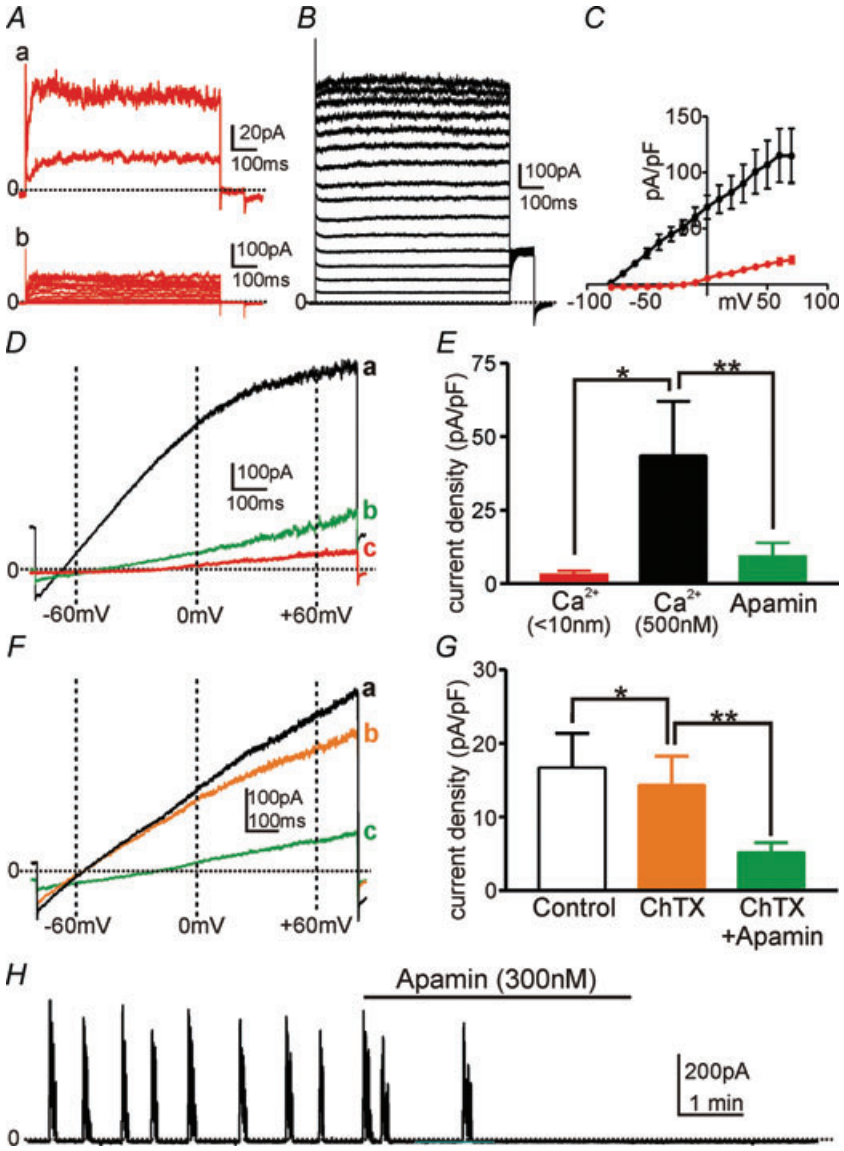

Figure 3. Ca^{2+}-activated K^+ currents in PDGFRα^+ cells
A and *B*, PDGFRα^+ cells were depolarized with step potentials from a holding potential of −80 mV with low Ca^{2+} (<10 nM) pipette solution 1 (*A*) or 500 nM Ca^{2+} pipette solution 2 (*B*). *Aa*, currents evoked by 800 ms steps to 0 mV (lower trace) and +40 mV (upper trace) in a cell with low Ca^{2+} (<10 nM; solution 1). Depolarization elicited small time-dependent currents and a noisy current at more positive potentials. *Ab* shows a family of currents evoked by 800 ms steps from −80 mV to +70 mV in 10 mV increments in a cell with low Ca^{2+} (<10 nM; solution 1). At the end of step depolarizations, potential was returned briefly to −40 mV before stepping back to the holding potential. Small time-dependent outward currents were evoked at potentials positive to −20 mV. *B*, currents evoked by steps from −80 mV to +70 mV (800 ms in 10 mV increments) in cells with 500 nM Ca^{2+} (solution 2). Large amplitude, time-independent outward currents developed in cells with increased $[Ca^{2+}]_i$. *C*, summary of current density as a function of test potential in cells with low Ca^{2+} (red line, $n = 4$) and 500 nM Ca^{2+} pipette solutions (black line, $n = 4$). *D*, ramp protocols (−80 to +80 mV, rate-of-rise = 0.17 mV ms^{-1}) were applied to PDGFRα^+ cells in whole cell configuration with pipette solutions containing: 500 nM Ca^{2+} (*a*), 500 nM Ca^{2+} after apamin (300 nM) (*b*), and low Ca^{2+} (<10 nM) (*c*). Cells with 500 nM Ca^{2+} solution developed large, apamin-sensitive outward currents. Currents were due to a K^+ conductance as apparent from leftward shift in reversal potential. Note inward rectification common to SK3 currents due to block by internal Mg^{2+} at depolarized potentials (Ledoux *et al.* 2008). Apamin reduced the outward current activated by high Ca^{2+} (*b*). With low Ca^{2+} (*c*) small amplitude linear currents were evoked in PDGFRα^+ cells. *E*, average current density at 0 mV in cells with low Ca^{2+} (red bar; 3.1 ± 2.6 pA pF^{-1}, $n = 16$), 500 nM Ca^{2+} (black bar, 43 ± 22 pA pF^{-1}, $n = 6$), and 500 nM Ca^{2+} and apamin (green bar, 9 ± 5.6 pA pF^{-1}, $n = 6$). 500 nM Ca^{2+} activated significant outward current (*$P = 0.0015$), and apamin (300 nM) reduced the current significantly (**$P < 0.0001$). *F*, responses to voltage

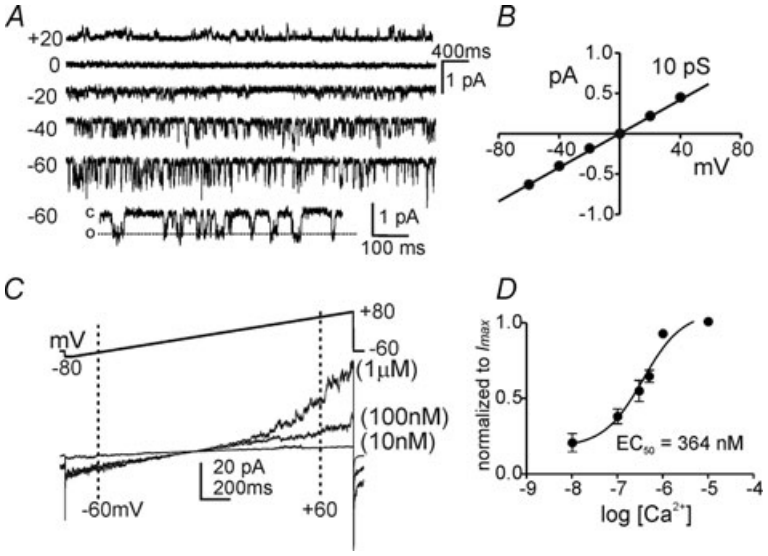

Figure 4. Ca^{2+}-dependent single channels in PDGFRα^+ cells
A, in symmetrical KCl (140 mM), excised inside-out (i-o) patches displayed single channel activity. The bath solution contained 100 nM Ca^{2+}. An expanded trace is shown at −60 mV to display channel openings. Closed (c) and open (o) states are denoted. Amplitude histograms (not shown) were constructed at various potentials and fitted amplitudes were plotted in *B* against test potentials. Linear fits yielded a single channel conductance of 10 pS. *C*, in symmetrical KCl i-o patches were ramped from −80 to 80 mV from a holding potential of −60 mV. [Ca^{2+}] in the bath solution (intracellular surface of patch) was changed from 10^{-8} to 10^{-5} M. *D*, calcium dose–response curve for current responses to ramped potentials in i-o patches. Currents at −60 mV were normalized to maximal current. Data were fitted with Boltzmann function and EC_{50} from 4 experiments averaged 364 ± 51 nM.

that antibodies for PDGFRα are robust, specific markers for FLCs (Iino *et al.* 2009). c-Kit-like immunoreactivity was not resolved in PDGFRα^+ cells, demonstrating that ICC and PDGFRα^+ cells are distinct populations of interstitial cells. We suggest replacing the vague term 'fibroblast-like cells' with 'PDGFRα^+ cells' to better identify this novel class of interstitial cells in the GI tract.

The role of PDGFRα^+ cells was previously unknown because cells were not identifiable in live whole muscles and no techniques were available to identify these cells in the mixed cell population resulting from enzymatic dispersion of muscles. One study examined electrical properties of cells from the murine intestine and identified a few cells that generated spontaneous transient outward currents (Goto *et al.* 2004). The authors suggested that these cells may be $CD34^+$ fibroblast-like cells described by morphologists. Another study investigated cells described as myofibroblasts in the suburothelium of the bladder (Wu *et al.* 2005). These cells displayed spontaneous transient depolarization and responded to purine agonists; however inward currents were evoked in contrast to the outward currents elicited by purines in PDGFRα^+ cells. It is at present unclear whether suburothelial myofibroblasts share common phenotypic characteristics with cells in the muscularis of visceral organs that have some common ultrastructural features. We used transgenic mice in which PDGFRα^+ cells were labelled constitutively with eGFP to identify cells within the tunica muscularis and study their responses to purines. We showed that PDGFRα^+ cells express appropriate receptors and effectors to receive and transduce purinergic neural signals. SK3 channels are highly expressed in PDGFRα^+ cells (Iino & Nojyo, 2009; and this study) and activation of these channels may contribute to the outward currents activated by purines in intact muscles in response to enteric inhibitory neurotransmission. Exposure of PDGFRα^+ cells to ATP, ADP or β-NAD, agonists for P2Y1 receptors, caused receptor-dependent activation of apamin-sensitive, outward currents in PDGFRα^+ cells. The current density of the apamin-sensitive, Ca^{2+}-activated K^+ conductance in PDGFRα^+ cells reached 100 pA pF^{-1} in some cells, suggesting dense expression of SK channels. Thus, PDGFRα^+ cells have specialized responsiveness to at least one class of enteric motor neurotransmitter and may contribute significantly to the purinergic component of enteric inhibitory neurotransmission.

Enteric inhibitory junction potentials (IJPs) were first described by Burnstock *et al.* (1963), providing a breakthrough in understanding the physiology of enteric

ramps (−80 to +80 mV, 0.17 mV ms^{-1}) in a cell dialysed with 500 nM Ca^{2+} (*a*). The cell was then exposed serially to charybdotoxin (ChTX; 200 nM; orange trace, *b*) and ChTX with apamin (300 nM; green trace, *c*). *G*, average current density at 0 mV under control conditions (500 nM Ca^{2+}; black bar; 16.6 ± 4.6 pA pF^{-1}, $n = 6$), ChTX (orange bar, 14.3 ± 3.9 pA pF^{-1}, $n = 6$), and ChTX and apamin (green bar, 5.2 ± 1.3 pA pF^{-1}, $n = 6$). ChTX reduced current (*$P = 0.0488$), with greater reduction at positive potentials, little effect at negative potentials, and little or no change in reversal potential. Apamin added with ChTX further reduced current (**$P = 0.0406$) and shifted reversal potential in the positive direction. *H*, some PDGFRα^+ cells generated STOCs with average amplitude of 42 ± 13.8 pA pF^{-1} and frequency of STOC complexes of 3.2 ± 0.8 min^{-1}. Cells were dialysed with low Ca^{2+} (solution 1) in these experiments; actual frequency of cells that generate STOCs could be much higher with physiological Ca^{2+} concentrations. Apamin (300 nM) blocked STOCs completely ($n = 4$).

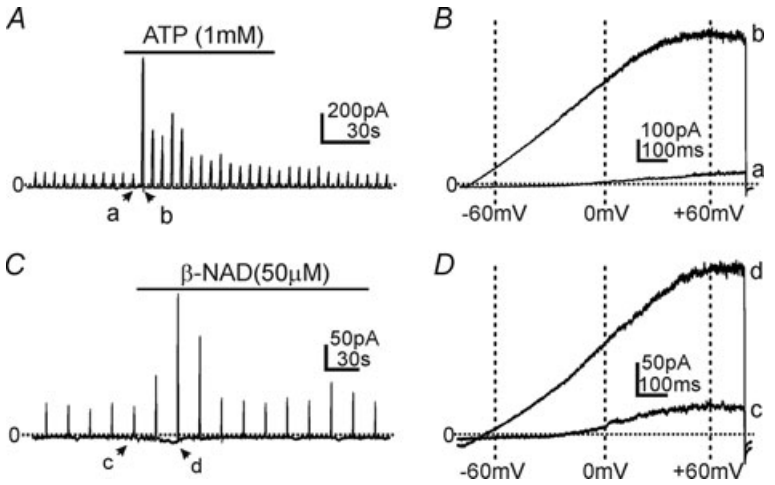

Figure 5. Activation of outward current by purines in PDGFRα^+ cells
A–D, ramped potentials (−80 to +80 mV, 0.17 mV ms^{-1}) were applied to PDGFRα^+ cells in the whole cell configuration (cells dialysed with solution 1). ATP (1 mM) and β-NAD (50 μM) (bars in *A* and *C*, respectively) elicited large outward currents (ATP elicited current density; 82 ± 26.9 pA pF^{-1}, $n = 16$, β-NAD elicited current density; 129 ± 101 pA pF^{-1}, $n = 3$). Responses to single voltage ramps (denoted as *a* and *b* or *c* and *d*; before and in the presence of the purine, respectively) are shown in *B* and *D*. The outward currents activated immediately upon application of the purines but deactivated in spite of continued exposure to ATP or β-NAD.

motor regulation. Together with nitric oxide, purinergic regulation is responsible for the descending inhibition phase of the peristaltic reflex (Bayliss & Starling, 1899) and tonic neural inhibition that dampens the intrinsic excitability of gastrointestinal smooth muscles (Wood, 1972). ATP, or a related purine, was deduced to be a primary neurotransmitter mediating enteric inhibitory responses (Burnstock *et al.* 1970), and the bee venom toxin, apamin, apamin, was shown to block IJPs elicited by purinergic nerve stimulation (Banks *et al.* 1979) and cause significant depolarization and increased excitability of colonic muscles (Mutafova-Yambolieva *et al.* 2007). Recent experiments have suggested that the purinergic inhibitory response is mediated by P2Y1 receptors because these receptors are expressed in GI muscles (Giaroni *et al.* 2002; Monaghan *et al.* 2006) and responses are blocked by selective P2Y1 antagonists (Gallego *et al.* 2006; Mutafova-Yambolieva *et al.* 2007). Most investigators have

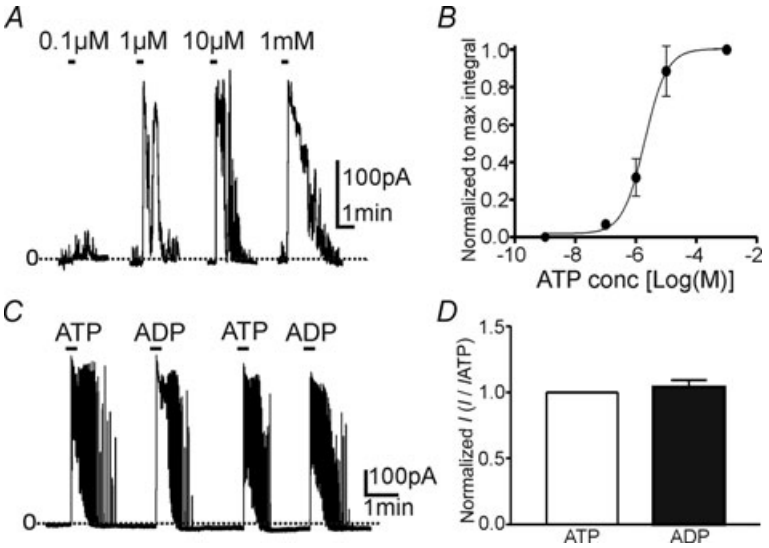

Figure 6. Effects of ATP were concentration dependent and repeatable
A, brief exposures (20 s) to ATP (0.1 μM, 1 μM, 10 μM and 1 mM) at a holding potential of −50 mV (approximate resting potential of murine colonic muscles) caused large outward currents, resolved at 0.1 μM and nearly maximal at 10 μM. *B*, ATP concentration *vs.* current response in 6 cells. The *X*-axis is the log of ATP concentration (M), and the *Y*-axis is the integral of ATP response current (area under the curve; AUC) normalized to the maximum response integral. Data were fitted with a Boltzmann function and EC_{50} was calculated to be 1.96 μM (Hill slope = 1.19). Averaged AUC at maximal ATP concentration (1 mM) was 55.19 ± 33.1 pA min ($n = 6$). *C* and *D*, outward currents elicited in a PDGFRα^+ cell by alternating exposures to ATP (10 μM) and ADP (10 μM). ATP and ADP had similar effects and repetitive application yielded reproducible responses. Note responses were often STOC-like and often extended past the period of exposure. *D*, averaged current responses to ATP and ADP in 7 cells. There were no significant difference in maximum current elicited by either ATP and ADP (ATP = 47.8 ± 20.0 pA pF^{-1} and ADP = 47.8 ± 20.3 pA pF^{-1}; $P = 0.4337$) or in integrated current responses (ATP = 165.9 ± 82.7 pA min and ADP = 133.5 ± 60.1 pA min; $P = 0.6416$; $n = 7$).

assumed that purinergic responses are mediated by ATP binding to SMC receptors (Vogalis & Goyal, 1997; Koh *et al.* 1997; Bayguinov *et al.* 2000). However, as authors of some of these studies, we were struck by the relatively small current density attributable to SK currents in SMCs, the large concentrations of ATP required to evoke responses, and the inability to elicit SK current responses to purines unless the permeabilized patch technique was used. It is unclear how SMCs could generate the large and fast outward current necessary to produce purinergic IJPs in intact muscles, which are tens of millivolts in amplitude with rates-of-rise approaching 0.5 mV s^{-1}. In the present study we confirmed the low current density responses in SMCs compared to the large amplitude responses in PDGFRα^+ cells. At −50 mV (which approximates resting potentials of colonic muscles) we were able to resolve minimal net outward currents in response to relatively high concentrations of ATP, and some cells showed small inward currents in response to ATP. In cells with net outward current responses, the current density activated by ATP in SMCs was about 1–2% of the current density in PDGFRα^+ cells. The pharmacology of the large outward Ca^{2+}-dependent currents activated by purines in PDGFRα^+ cells is consistent with the pharmacology of fast, purinergic IJPs in intact murine colonic muscles (see Mutafova-Yambolieva *et al.* 2007). Along with anatomical features (e.g. proximity of PDGFRα^+ cells to enteric nerve terminals and gap junctions with SMCs) our data suggest that these cells mediate a significant component of the purinergic postjunctional response in colonic muscles.

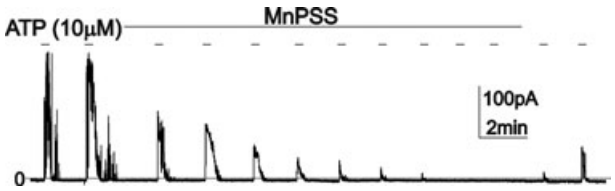

Figure 8. Currents activated by ATP were Ca^{2+} dependent
ATP (10 μM) responses were evoked by repetitive exposures in CaPSS bath solution. Switching the external solution to MnPSS (black bar), completely replacing extracellular Ca^{2+}, progressively blocked ATP responses (e.g. average outward current in CaPSS: 37.2 ± 10.4 pA pF^{-1}; after switching to MnPSS: 0.67 ± 0.72 pA, $n = 5$; $P = 0.0213$). ATP evoked currents were slowly restored after replacement of CaPSS.

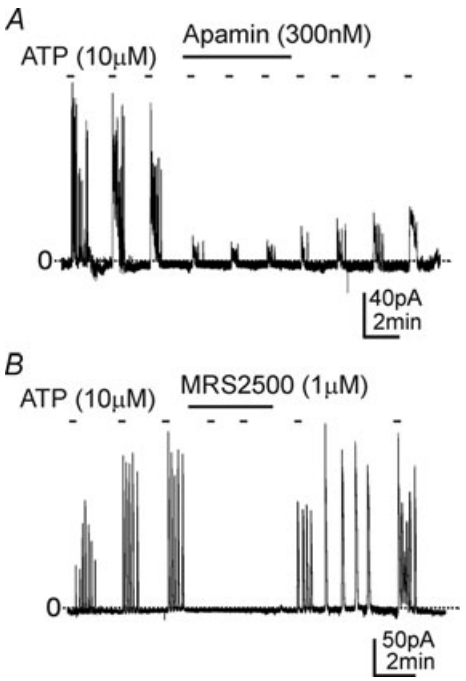

Figure 7. Blockade of ATP responses by SK channel blocker and P2Y1 antagonist
A, brief exposures (20 s) to ATP (10 μM) elicited reproducible large outward currents in PDGFRα^+ cells (average 26.0 ± 5.8 pA pF^{-1}, $n = 6$) that were reduced by apamin (300 nM) (7.8 ± 6.1 pA pF^{-1}, $n = 6$; $P = 0.0008$). *B*, MRS2500 (1 μM) blocked outward currents elicited by ATP (control ATP response 37.5 ± 19.2 pA pF^{-1}; after MRS2500 1.0 ± 1.0 pA pF^{-1}, $n = 8$; $P < 0.0001$).

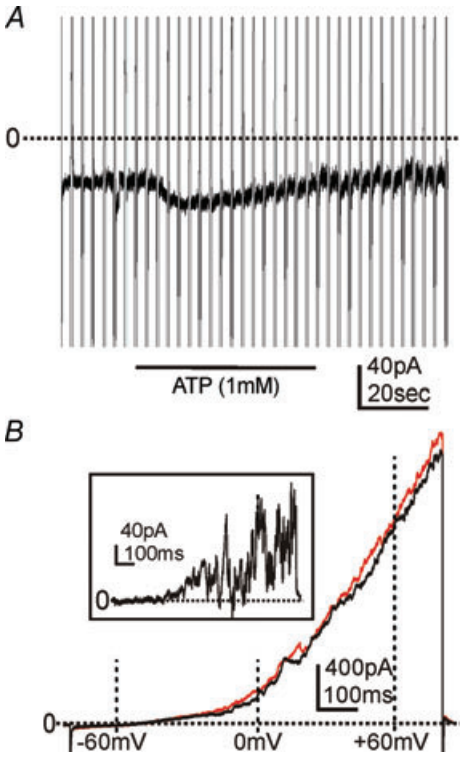

Figure 9. Responses of smooth muscle cells to ATP
ATP (1 mM) produced very small current responses in smooth muscle cells. *A* and *B*, ramp protocols (−80 to +80 mV, 0.17 mV ms^{-1}) were applied to smooth muscle cells in perforated patch whole-cell configuration. *A*, ATP elicited small inward currents in some cells (*A*), and small outward currents were evoked in other cells. *B*, responses to ramps before (black) and in the presence of ATP (1 mM; red). Inset shows a difference current from subtracting current responses. Small outward currents were evoked at positive potentials, but outward current at −50 mV was unresolvable.

The target and transmitter(s) for purinergic neurotransmission in visceral smooth have been controversial. GI SMCs express both P2X (Bo *et al.* 2003; Zhang & Paterson, 2005; Lee *et al.* 2005) and P2Y (Giaroni *et al.* 2002; Monaghan *et al.* 2006; Gallego *et al.* 2006; Mutafova-Yambolieva *et al.* 2007) receptors, so responses of these cells to purines are potentially complex, resulting in depolarization, hyperpolarization, or multi-phasic responses (see Monaghan *et al.* 2006). In previous studies we reported activation of channels in murine colonic muscles in response to P2Y receptor agonists that were consistent with the properties of SK channels. P2Y agonists also elicited Ca^{2+} puffs in colonic SMCs of mice and guinea pigs (Koh *et al.* 1997; Kong *et al.* 2000, Bayguinov *et al.* 2000) associated with spontaneous transient outward currents. Expression of SK isoforms in murine colonic muscles was also previously studied (Ro *et al.* 2001), but without consideration of expression of specific isoforms in PDGFRα^+ cells. All three SK channel isoforms were identified in extracts of whole muscles, and SK2 was the dominant isoform in SMCs. PDGFRα^+ cells are estimated to represent less than 10% of the total cellular volume of the tunica muscularis. There was significant expression of SK3 (mRNA and protein in these cells). Thus, most SK3 expression in whole tissue extracts may be due to PDGFRα^+ cells. Expression of other SK isoforms in these cells has not yet been analysed. Thus, SK channels are present in GI muscles, and specific isoforms vary in SMCs and PDGFRα^+ cells. Experiments using isoform-specific knockouts of SK channels may help determine if SK3 channels are dominant in purinergic responses.

Ca^{2+}-activated K^+ channels in addition to apamin-sensitive SK channels may be expressed in PDGFRα^+ cells. ChTX reduced the amplitude of the current activated by dialysis of cells with 500 nM Ca^{2+}. ChTX is capable of blocking both SK4 (IK) and BK channels. We have not yet analysed extracts of PDGFRα^+ cells for transcripts of additional SK and BK isoforms, and further pharmacological studies using more specific blockers of IK and BK to determine the relative contributions of these channels to whole cell currents were not performed. ChTX caused significant reduction in outward current at 0 mV and at more positive potentials; however, it was difficult to resolve effects of ChTX at −50 mV and at more negative potentials (see Fig. 3). The increasing effectiveness of ChTX to block outward currents in PDGFRα^+ cells may be due to the voltage-dependent properties of BK channels (i.e. more BK channels were activated at positive potentials and thus this conductance contributed more to net outward currents, possibly the noisy current observed in response to voltage steps, at positive membrane potentials). GI smooth muscle syncytia operate at negative potentials, even during periods of excitation. Enteric inhibitory responses are elicited at quite negative potentials (Mutafova-Yambolieva *et al.* 2007); for example purinergic IJPs are initiated typically from about −50 mV (resting potential) and hyperpolarize the smooth muscles by 20–30 mV. Thus, lack of resolvable ChTX-sensitive outward currents in PDGFRα^+ cells at negative potentials suggests that contributions to the IJP from activation of IK or BK in these cells may be minor.

It is unlikely that purinergic neurotransmission is mediated by ICC since these responses were intact in gastric muscles of W/W^V mice, which lack most intramuscular ICC (Burns *et al.* 1996; Sergeant *et al.* 2002). Purinergic responses were actually increased in W/W^V mice, and it is possible that ICC might contribute to the metabolism of purines released from neurons or restrict the diffusion of purine transmitters to surrounding cells. Remodelling of the neuromuscular apparatus including upregulation of P2Y receptor expression in W/W^V mice may also affect responses (Sergeant *et al.* 2002). Taken together, available data do not rule out a postjunctional role for ICC and SMCs in purinergic neurotransmission, but these cells appear to be less likely to have primary responsibility for generating fast IJPs, which is the signature response of purinergic neurotransmission in the GI tract (Burnstock *et al.* 1963, Gallego *et al.* 2006; Mutafova-Yambolieva *et al.* 2007). Our findings suggest that PDGFRα^+ cells are likely postjunctional targets mediating purinergic enteric inhibitory responses. A more definitive test of the role of PDGFRα^+ cells would be to inhibit their development or selectively lesion these cells in adult tissues, strategies we employed to link ICC to functional roles in nitrergic and cholinergic neurotransmission (e.g. Burns *et al.* 1996; Ward *et al.* 2000). Unfortunately, the equivalent of Kit mutants (e.g. W/W^V) with selective ICC lesions does not appear likely for PDGFRα, because deactivation of this receptor is developmentally lethal (Hamilton *et al.* 2003).

In summary, PDGFRα^+ cells form prominent networks of interstitial cells distinct from ICC in GI muscles. Localization of PDGFRα^+ cells near terminals of enteric motor neurons and gap junction connectivity with SMCs suggest a possible role for these cells in motor neurotransmission. Molecular analysis shows that these cells express receptors and effectors consistent with transduction of purinergic neurotransmitters. Large Ca^{2+}-dependent currents are prominent in PDGFRα^+ cells, and this conductance is activated by P2Y1 receptor agonists. Apamin and the P2Y1 selective antagonist MRS2500 blocked the activation of currents by purines. ATP evoked small responses in SMCs that would be unlikely to generate purinergic IJPs in intact muscles. Our data suggest that PDGFRα^+ cells are excitable cells in the tunica muscularis that transduce inputs from enteric motor neurons and may be primary mediators of enteric inhibitory neural control of GI motility. Techniques described in this paper make it possible to investigate

the role of this novel class of interstitial cells, which are common in a variety of smooth muscles.

References

Banks BE, Brown C, Burgess GM, Burnstock G, Claret M, Cocks TM & Jenkinson DH (1979). Apamin blocks certain neurotransmitter-induced increases in potassium permeability. *Nature* **282**, 415–417.

Barfod ET, Moore AL & Lidofsky SD (2001). Cloning and functional expression of a liver isoform of the small conductance Ca^{2+}-activated K^+ channel SK3. *Am J Physiol Cell Physiol* **280**, C836–C842.

Bayguinov O, Hagen B, Bonev AD, Nelson MT & Sanders KM (2000). Intracellular calcium events activated by ATP in murine colonic myocytes. *Am J Physiol Cell Physiol* **279**, C126–C135.

Bayliss WM & Starling EH (1899). The movements and innervation of the small intestine. *J Physiol* **24**, 99–143.

Blatz AL & Magleby KL (1986). Single apamin-blocked Ca-activated K^+ channels of small conductance in cultured rat skeletal muscle. *Nature* **323**, 718–720.

Bo X, Kim M, Nori SL, Schoepfer R, Burnstock G & North RA (2003). Tissue distribution of P2X4 receptors studied with an ectodomain antibody. *Cell Tissue Res* **313**, 159–165.

Bredt DS, Hwang PM & Snyder SH (1990). Localization of nitric oxide synthase indicating a neural role for nitric oxide. *Nature* **347**, 768–770.

Burns AJ, Lomax AE, Torihashi S, Sanders KM & Ward SM (1996). Interstitial cells of Cajal mediate inhibitory neurotransmission in the stomach. *Proc Natl Acad Sci U S A* **93**, 12008–12013.

Burnstock G, Campbell G, Bennett M & Holman M (1963). Inhibition of the smooth muscle of the taenia coli. *Nature* **200**, 581–582.

Burnstock G, Campbell G, Satchell D & Smythe A (1970). Evidence that adenosine triphosphate or a related nucleotide is the transmitter substance released by non-adrenergic inhibitory nerves in the gut. *Br J Pharmacol* **40**, 668–688.

Fujita A, Takeuchi T, Jun H & Hata F (2003). Localization of Ca^{2+}-activated K^+ channel, SK3, in fibroblast-like cells forming gap junctions with smooth muscle cells in the mouse small intestine. *J Pharmacol Sci* **92**, 35–42.

Gallego D, Hernández P, Clavé P & Jiménez M (2006). P2Y1 receptors mediate inhibitory purinergic neuromuscular transmission in the human colon. *Am J Physiol Gastrointest Liver Physiol* 291, G584–G594.

Giaroni C, Knight GE, Ruan HZ, Glass R, Bardini M, Lecchini S, Frigo G & Burnstock G (2002). P2 receptors in the murine gastrointestinal tract. *Neuropharmacology* **43**, 1313–1323.

Goto K, Matsuoka S & Noma A (2004). Two types of spontaneous depolarizations in the interstitial cells freshly prepared from the murine small intestine. *J Physiol* **559**, 411–422.

Hamilton TG, Klinghoffer RA, Corrin PD & Soriano P (2003). Evolutionary divergence of platelet-derived growth factor α receptor signaling mechanisms. *Mol Cell Biol* **23**, 4013–4025.

Horiguchi K & Komuro T (2000). Ultrastructural observations of fibroblast-like cells forming gap junctions in the W/W(nu) mouse small intestine. *J Auton Nerv Syst* **80**, 142–147.

Hwang SJ, Blair PJ, Britton FC, O'Driscoll KE, Hennig G, Bayguinov YR, Rock JR, Harfe BD, Sanders KM & Ward SM (2009). Expression of anoctamin 1/TMEM16A by interstitial cells of Cajal is fundamental for slow wave activity in gastrointestinal muscles. *J Physiol* **587**, 4887–4904.

Iino S, Horiguchi K, Horiguchi S & Nojyo Y (2009). c-Kit-negative fibroblast-like cells express platelet-derived growth factor receptor α in the murine gastrointestinal musculature. *Histochem Cell Biol* **131**, 691–702.

Iino S & Nojyo Y (2009). Immunohistochemical demonstration of c-Kit-negative fibroblast-like cells in murine gastrointestinal musculature. *Arch Histol Cytol* **72**, 107–115.

Klemm MF & Lang RJ (2002). Distribution of Ca^{2+}-activated K^+ channel (SK2 and SK3) immunoreactivity in intestinal smooth muscles of the guinea-pig. *Clin Exp Pharmacol Physiol* **29**, 18–25.

Koh SD, Dick GM & Sanders KM (1997). Small-conductance Ca^{2+}-dependent K^+ channels activated by ATP in murine colonic smooth muscle. *Am J Physiol Cell Physiol* **273**, C2010–C2021.

Komuro T & Seki K, Horiguchi K (1999). Ultrastructural characterization of the interstitial cells of Cajal. *Arch Histol Cytol* **62**, 295–316.

Kong ID, Koh SD & Sanders KM (2000). Purinergic activation of spontaneous transient outward currents in guinea pig taenia colonic myocytes. *Am J Physiol Cell Physiol* **278**, C352–C362.

Ledoux J, Bonev AD & Nelson MT (2008). Ca^{2+}-activated K^+ channels in murine endothelial cells: block by intracellular calcium and magnesium. *J Gen Physiol* **131**, 125–135.

Ledoux J, Werner ME, Brayden JE & Nelson MT (2006). Calcium-activated potassium channels and the regulation of vascular tone. *Physiology (Bethesda)* **21**, 69–78.

Lee HK, Ro S, Keef KD, Kim YH, Kim HW, Horowitz B & Sanders KM (2005). Differential expression of P2X-purinoceptor subtypes in circular and longitudinal muscle of canine colon. *Neurogastroenterol Motil* **17**, 575–584.

Monaghan KP, Koh SD, Ro S, Yeom J, Horowitz B & Sanders KM (2006). Nucleotide regulation of the voltage-dependent nonselective cation conductance in murine colonic myocytes. *Am J Physiol Cell Physiol* **291**, C985–C994.

Mutafova-Yambolieva VN, Hwang SJ, Hao X, Chen H, Zhu MX, Wood JD, Ward SM & Sanders KM (2007). β-Nicotinamide adenine dinucleotide is an inhibitory neurotransmitter in visceral smooth muscle. *Proc Natl Acad Sci U S A* **104**, 16359–16364.

Ro S, Hatton WJ, Koh SD & Horowitz B (2001). Molecular properties of small-conductance Ca^{2+}-activated K^+ channels expressed in murine colonic smooth muscle. *Am J Physiol Gastrointest Liver Physiol* **281**, G964–G973.

Sanders KM (1996). A case for interstitial cells of Cajal as pacemakers and mediators of neurotransmission in the gastrointestinal tract. *Gastroenterology* **111**, 492–515.

Sergeant GP, Large RJ, Beckett EA, McGeough CM, Ward SM & Horowitz B (2002). Microarray comparison of normal and W/W^V mice in the gastric fundus indicates a supersensitive phenotype. *Physiol Genomics* **11**, 1–9.

Vanderwinden JM, Rumessen JJ, de Kerchove d'Exaerde A Jr, Gillard K, Panthier JJ, de Laet MH & Schiffmann SN (2002). Kit-negative fibroblast-like cells expressing SK3, a Ca^{2+}-activated K^+ channel, in the gut musculature in health and disease. *Cell Tissue Res* **310**, 349–358.

Vanderwinden JM, Rumessen JJ, De Laet MH, Vanderhaeghen JJ & Schiffmann SN (1999). CD34+ cells in human intestine are fibroblasts adjacent to, but distinct from, interstitial cells of Cajal. *Lab Invest* **79**, 59–65.

Vanderwinden JM, Rumessen JJ, De Laet MH, Vanderhaeghen JJ & Schiffmann SN (2000). CD34 immunoreactivity and interstitial cells of Cajal in the human and mouse gastrointestinal tract. *Cell Tissue Res* **302**, 145–153.

Vogalis F & Goyal RK (1997). Activation of small conductance Ca^{2+}-dependent K^+ channels by purinergic agonists in smooth muscle cells of the mouse ileum. *J Physiol* **502**, 497–508.

Ward SM, Beckett EA, Wang X, Baker F, Khoyi M & Sanders KM (2000). Interstitial cells of Cajal mediate cholinergic neurotransmission from enteric motor neurons. *J Neurosci* **20**, 1393–1403.

Ward SM, Xue C, Shuttleworth CW, Bredt DS, Snyder SH & Sanders KM (1992). NADPH diaphorase and nitric oxide synthase colocalization in enteric neurons of canine proximal colon. *Am J Physiol Gastrointest Liver Physiol* **263**, G277–G284.

Weihe E, Tao-Cheng JH, Schäfer MK, Erickson JD & Eiden LE (1996). Visualization of the vesicular acetylcholine transporter in cholinergic nerve terminals and its targeting to a specific population of small synaptic vesicles. *Proc Natl Acad Sci U S A* **93**, 3547–3552.

Wood JD (1972). Excitation of intestinal muscle by atropine, tetrodotoxin, and xylocaine. *Am J Physiol* **222**, 118–125.

Wu C, Sui GP & Fry CH (2005). Purinergic regulation of guinea pig suburothelial myofibroblasts. *J Physiol* **559**, 231–243.

Zhang Y & Paterson WG (2005). Excitatory purinergic neurotransmission in smooth muscle of guinea-pig taenia caeci. *J Physiol* **563**, 855–865.

Zhou DS & Komuro T (1992). The cellular network of interstitial cells associated with the deep muscular plexus of the guinea pig small intestine. *Anat Embryol (Berl)* **186**, 519–527.

Zhu MH, Kim TW, Ro S, Yan W, Ward SM, Koh SD & Sanders KM (2009). A Ca^{2+}-activated Cl^- conductance in interstitial cells of Cajal linked to slow wave currents and pacemaker activity. *J Physiol* **587**, 4905–4918.

Author contributions

M.K.: conception and design of experiments, collection, analysis and interpretation of data, and revision of the paper critically for important intellectual content. H.Z.: collection, analysis and interpretation of data. L.D.: collection, analysis and interpretation of data. S.W.: Conception and design of experiments and revision of the paper critically for important intellectual content. S.D.K.: conception and design of experiments, analysis of data and revision of the paper critically for important intellectual content. K.S.: conception and design of experiments, drafting of the article and revision of it critically for important intellectual content. All authors approved of the final version of the manuscript.

Acknowledgements

This work was supported as a Pilot Project as part of P01 DK41315 to KS, SDK and SW and by institutional support funds from the University of Nevada, Reno to supplement DK41315. Images were collected using a Zeiss LSM510 confocal microscope and a core morphology facility obtained with support from NIH1 S10 RR16871 and DK41315. The authors are grateful to Dr Sung Jin Hwang for calculations of inhibitory junction potential dV/dt.